Supplementary Information: Revealing the Materials Genome of Superhard High-Entropy Diborides via the Hybrid Data-driven and Knowledge-enabled Mode

Jiaqi Lu[a,b], Fengpei Zhang[a], William Yi Wang[a,b,*], Gang Yao[a], Xingyu Gao[c], Ya Liu[a,b], Zhi Zhang [d], Jun Wang[a,b], Yiguang Wang[e], Xiubing Liang[f], Haifeng Song[c,*], Jinshan Li[a,b,*], Pingxiang Zhang[a]

[a]State Key Laboratory of Solidification Processing, Northwestern Polytechnical University, Xi'an, 710072, China

[b]Innovation Center, NPU Chongqing, Chongqing 401135, China

[c]Laboratory of Computational Physics, Institute of Applied Physics and Computational Mathematics, Beijing 100088, China

[d]Digital Intelligence Technology Innovation Center, Central Research, BAOSHAN IRON & STEEL CO, LTD. Shanghai, 201900, China

[e]Institute of Advanced Structure Technology, Beijing Institute of Technology, Haidian District, Beijing, 100081, China

[f]Defense Innovation Institute, Academy of Military Sciences of the PLA of China, Beijing 100071, China

* Corresponding author.

E-mail: wywang@nwpu.edu.cn; Song_haifeng@ iapcm.ac.cn; ljsh@nwpu.edu.cn

Supplementary Note 1: HEBs Database

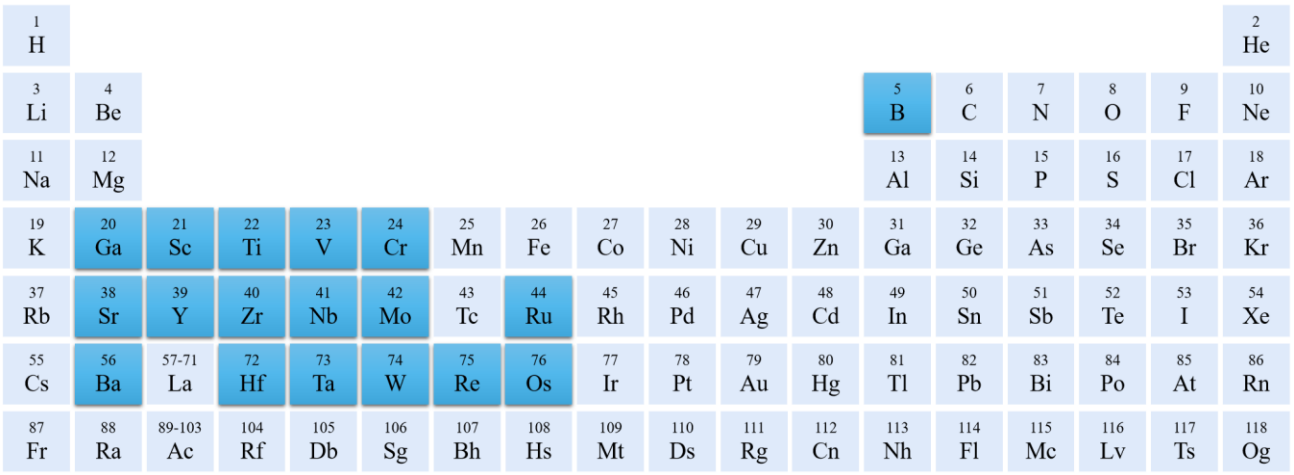

Figure S1. Distribution of the elements (dark blue) in HEBs dataset collected by experiment and calculate report.

Table S1. Dataset for high-entropy boride ceramics used included Vickers hardness (Hv), load, VEC, EWF, EWF^6.

Index	Compositions	Load/ (kg)	EWF^6	EWF	VEC	Hardness/(GPa)	Ref
1	$(Hf_{0.2}Zr_{0.2}Ta_{0.2}Nb_{0.2}Ti_{0.2})B_2$	0.2	6825.373163	4.35533	10.4	25.61	[1]
2	$(Hf_{0.2}Zr_{0.2}Ta_{0.2}Nb_{0.2}Ti_{0.2})B_2$	1	6825.373163	4.35533	10.4	22.44	[1]
3	$(Hf_{0.2}Zr_{0.2}Ta_{0.2}Nb_{0.2}Ti_{0.2})B_2$	0.2	6825.373163	4.35533	10.4	26.82	[1]
4	$(Hf_{0.2}Zr_{0.2}Ta_{0.2}Nb_{0.2}Ti_{0.2})B_2$	0.2	6825.373163	4.35533	10.4	25.4	[2]
5	$(Hf_{0.2}Zr_{0.2}Ta_{0.2}Nb_{0.2}Ti_{0.2})B_2$	0.2	6825.373163	4.35533	10.4	25.2	[2]
6	$(Hf_{0.2}Zr_{0.2}Ta_{0.2}Nb_{0.2}Ti_{0.2})B_2$	0.2	6825.373163	4.35533	10.4	24.3	[2]
7	$(Hf_{0.2}Zr_{0.2}Ta_{0.2}Nb_{0.2}Ti_{0.2})B_2$	0.2	6825.373163	4.35533	10.4	25.3	[3]
8	$(Hf_{0.2}Zr_{0.2}Ta_{0.2}Nb_{0.2}Ti_{0.2})B_2$	0.2	6825.373163	4.35533	10.4	26.2	[4]
9	$(Hf_{0.2}Zr_{0.2}Ta_{0.2}Nb_{0.2}Ti_{0.2})B_2$	1	6825.373163	4.35533	10.4	22	[5]
10	$(Hf_{0.2}Zr_{0.2}Ta_{0.2}Nb_{0.2}Ti_{0.2})B_2$	5	6825.373163	4.35533	10.4	20.2	[5]
11	$(Hf_{0.2}Zr_{0.2}Ta_{0.2}Nb_{0.2}Ti_{0.2})B_2$	1	6825.373163	4.35533	10.4	21	[6]
12	$(Hf_{0.2}Zr_{0.2}Ta_{0.2}Nb_{0.2}Ti_{0.2})B_2$	0.5	6825.373163	4.35533	10.4	23.5	[6]
13	$(Hf_{0.2}Zr_{0.2}Ta_{0.2}Nb_{0.2}Ti_{0.2})B_2$	0.2	6825.373163	4.35533	10.4	25.2	[6]

14	$(Hf_{0.2}Zr_{0.2}Ta_{0.2}Nb_{0.2}Ti_{0.2})B_2$	0.1	6825.373163	4.35533	10.4	29.1	[6]
15	$(Hf_{0.2}Zr_{0.2}Ta_{0.2}Nb_{0.2}Ti_{0.2})B_2$	0.05	6825.373163	4.35533	10.4	33.1	[6]
16	$(Hf_{0.2}Zr_{0.2}Ta_{0.2}Mo_{0.2}Ti_{0.2})B_2$	1	7015.601076	4.37533	10.6	25	[6]
17	$(Hf_{0.2}Zr_{0.2}Ta_{0.2}Mo_{0.2}Ti_{0.2})B_2$	0.5	7015.601076	4.37533	10.6	28.3	[6]
18	$(Hf_{0.2}Zr_{0.2}Ta_{0.2}Mo_{0.2}Ti_{0.2})B_2$	0.2	7015.601076	4.37533	10.6	30.6	[6]
19	$(Hf_{0.2}Zr_{0.2}Ta_{0.2}Mo_{0.2}Ti_{0.2})B_2$	0.1	7015.601076	4.37533	10.6	37.3	[6]
20	$(Hf_{0.2}Zr_{0.2}Ta_{0.2}Mo_{0.2}Ti_{0.2})B_2$	0.05	7015.601076	4.37533	10.6	38.6	[6]
21	$(Hf_{0.2}Zr_{0.2}Mo_{0.2}Nb_{0.2}Ti_{0.2})B_2$	0.2	7047.766528	4.378667	10.6	26.3	[7]
22	$(Hf_{0.2}Zr_{0.2}Mo_{0.2}Nb_{0.2}Ti_{0.2})B2$	0.2	7047.766528	4.378667	10.6	26.3	[8]
23	$(Hf_{0.2}Zr_{0.2}Mo_{0.2}Nb_{0.2}Ti_{0.2})B_2$	0.2	7047.766528	4.378667	10.6	25.9	[8]
24	$(Hf_{0.2}Mo_{0.2}Ta_{0.2}Nb_{0.2}Ti_{0.2})B_2$	0.2	7177.513015	4.392	10.8	27	[7]
25	$(Hf_{0.2}Mo_{0.2}Ta_{0.2}Nb_{0.2}Ti_{0.2})B_2$	0.2	7177.513015	4.392	10.8	25.9	[8]
26	$(Hf_{0.2}Zr_{0.2}W_{0.2}Mo_{0.2}Ti_{0.2})B_2$	0.2	7210.226769	4.39533	10.8	29.4	[9]
27	$(Hf_{0.2}Zr_{0.2}W_{0.2}Mo_{0.2}Ti_{0.2})B_2$	0.5	7210.226769	4.39533	10.8	27.3	[6]
28	$(Hf_{0.2}Zr_{0.2}W_{0.2}Mo_{0.2}Ti_{0.2})B_2$	0.2	7210.226769	4.39533	10.8	30.9	[6]
29	$(Hf_{0.2}Zr_{0.2}W_{0.2}Mo_{0.2}Ti_{0.2})B_2$	0.1	7210.226769	4.39533	10.8	35	[6]
30	$(Hf_{0.2}Zr_{0.2}W_{0.2}Mo_{0.2}Ti_{0.2})B_2$	0.05	7210.226769	4.39533	10.8	40	[6]
31	$(Hf_{0.2}Zr_{0.2}Ta_{0.2}Cr_{0.2}Ti_{0.2})B_2$	0.2	6951.770746	4.36867	10.6	28.3	[8]
32	$(Hf_{0.2}Zr_{0.2}Ta_{0.2}Cr_{0.2}Ti_{0.2})B_2$	1	6951.770746	4.36867	10.6	25.4	[6]
33	$(Hf_{0.2}Zr_{0.2}Ta_{0.2}Cr_{0.2}Ti_{0.2})B_2$	0.5	6951.770746	4.36867	10.6	27.6	[6]
34	$(Hf_{0.2}Zr_{0.2}Ta_{0.2}Cr_{0.2}Ti_{0.2})B_2$	0.2	6951.770746	4.36867	10.6	32.9	[6]
35	$(Hf_{0.2}Zr_{0.2}Ta_{0.2}Cr_{0.2}Ti_{0.2})B_2$	0.1	6951.770746	4.36867	10.6	40.4	[6]
36	$(Hf_{0.2}Zr_{0.2}Ta_{0.2}Cr_{0.2}Ti_{0.2})B_2$	0.05	6951.770746	4.36867	10.6	48.3	[6]
37	$(Hf_{0.2}Zr_{0.2}Nb_{0.2}Mo_{0.2}Ta_{0.2})B_2$	0.2	6996.381711	4.37333	10.8	24	[10]
38	$(Hf_{0.2}Zr_{0.2}Nb_{0.2}Mo_{0.2}Ta_{0.2})B_2$	0.5	6996.381711	4.37333	10.8	22.5	[10]
39	$(Hf_{0.2}Zr_{0.2}Nb_{0.2}Mo_{0.2}Ta_{0.2})B_2$	1	6996.381711	4.37333	10.8	20	[10]
40	$(Ta_{0.2}Nb_{0.2}Zr_{0.2}Cr_{0.2}Ti_{0.2})B_2$	0.2	7210.226769	4.39533	10.8	27.8	[11]
41	$(Ta_{0.2}Nb_{0.2}Zr_{0.2}Cr_{0.2}Ti_{0.2})B_2$	0.3	7210.226769	4.39533	10.8	25.2	[11]

42	$(Ta_{0.2}Nb_{0.2}Zr_{0.2}Cr_{0.2}Ti_{0.2})B_2$	0.5	7210.226769	4.39533	10.8	23.8	[11]
43	$(Ta_{0.2}Nb_{0.2}Zr_{0.2}Cr_{0.2}Ti_{0.2})B_2$	1	7210.226769	4.39533	10.8	22	[11]
44	$(Ta_{0.167}Nb_{0.167}Zr_{0.}167Hf_{0.167}Ti_{0.167}Cr_{0.167})B_2$	0.2	7001.758705	4.37389	10.676	24.3	[11]
45	$(Ta_{0.167}Nb_{0.167}Zr_{0.167}Hf_{0.167}Ti_{0.167}Cr_{0.167})B_2$	0.3	7001.758705	4.37389	10.676	18.6	[11]
46	$(Hf_{0.2}Zr_{0.2}Ti_{0.2}V_{0.2}Ta_{0.2})B_2$	1	6825.373163	4.35533	10.4	23	[6]
47	$(Hf_{0.2}Zr_{0.2}Ti_{0.2}V_{0.2}Ta_{0.2})B_2$	0.5	6825.373163	4.35533	10.4	26.3	[6]
48	$(Hf_{0.2}Zr_{0.2}Ti_{0.2}V_{0.2}Ta_{0.2})B_2$	0.2	6825.373163	4.35533	10.4	28.3	[6]
49	$(Hf_{0.2}Zr_{0.2}Ti_{0.2}V_{0.2}Ta_{0.2})B_2$	0.1	6825.373163	4.35533	10.4	31.7	[6]
50	$(Hf_{0.2}Zr_{0.2}Ti_{0.2}V_{0.2}Ta_{0.2})B_2$	0.05	6825.373163	4.35533	10.4	37.3	[6]
51	$(Hf_{0.2}Zr_{0.2}Ti_{0.2}W_{0.2}Ta_{0.2})B_2$	1	6983.625139	4.372	10.6	25.4	[6]
52	$(Hf_{0.2}Zr_{0.2}Ti_{0.2}W_{0.2}Ta_{0.2})B_2$	0.5	6983.625139	4.372	10.6	28.3	[6]
53	$(Hf_{0.2}Zr_{0.2}Ti_{0.2}W_{0.2}Ta_{0.2})B_2$	0.2	6983.625139	4.372	10.6	34.8	[6]
54	$(Hf_{0.2}Zr_{0.2}Ti_{0.2}W_{0.2}Ta_{0.2})B_2$	0.1	6983.625139	4.372	10.6	41.8	[6]
55	$(Hf_{0.2}Zr_{0.2}Ti_{0.2}W_{0.2}Ta_{0.2})B_2$	0.05	6983.625139	4.372	10.6	45.8	[6]
56	HfB_2	0.03	6033.013892	4.26667	10	28.4	[12]
57	HfB_2	0.03	6033.013892	4.26667	10	28.44	[13]
58	HfB_2	5	6033.013892	4.26667	10	17.8	[14]
59	HfB_2	0.5	6033.013892	4.26667	10	21.2	[15]
60	HfB_2	1	6033.013892	4.26667	10	19.8	[16]
61	ZrB_2	0.01	6469.833352	4.31667	10	23	[17]
62	ZrB_2	0.03	6469.833352	4.31667	10	22.08	[18]
63	ZrB_2	0.05	6469.833352	4.31667	10	18	[17]
64	ZrB_2	0.1	6469.833352	4.31667	10	17	[17]
65	ZrB_2	0.2	6469.833352	4.31667	10	15.4	[19]
66	ZrB_2	0.3	6469.833352	4.31667	10	16.86	[20]
67	ZrB_2	0.5	6469.833352	4.31667	10	15.48	[21]
68	ZrB_2	0.5	6469.833352	4.31667	10	15.55	[20]

69	ZrB_2	1	6469.833352	4.31667	10	14.40±1.33	[21]
70	ZrB_2	1	6469.833352	4.31667	10	14.4	[22]
71	ZrB_2	1	6469.833352	4.31667	10	14.72	[20]
72	ZrB_2	5	6469.833352	4.31667	10	10.35	[23]
73	ZrB_2	5	6469.833352	4.31667	10	11.18	[23]
74	ZrB_2	5	6469.833352	4.31667	10	11.57	[23]
75	ZrB_2	5	6469.833352	4.31667	10	11.9	[24]
76	ZrB_{12}	0.5	7448.685379	4.41923	40	27	[18]
77	ZrB_{12}	0.05	7448.685379	4.41923	40	40	[25]
78	ZrB_{12}	0.05	7448.685379	4.41923	40	40.4	[26]
79	ZrB	0.03	5892.961182	4.25	7	35.3	[27]
80	TaB_2	0.2	7092.91911	4.38333	11	17.5	[19]
81	TaB_2	0.5	7092.91911	4.38333	11	25.6	[28]
82	TaB_2	1	7092.91911	4.38333	11	25.1	[29]
83	TaB	3	6775.409391	4.35	8	13.9	[30]
84	TaB	0.05	6775.409391	4.35	8	30.69	[13]
85	Ta_3B_2	0.05	6590.636787	4.33	21	27.16	[13]
86	Ta_3B_4	0.05	6910.056625	4.36429	27	32.85	[13]
87	NbB_2	0.03	7256.313856	4.4	11	25.5	[13]
88	NbB_2	0.03	7256.313856	4.4	11	25.5	[12]
89	NbB_2	0.1	7256.313856	4.4	11	20.25	[15]
90	NbB_2	0.5	7256.313856	4.4	11	20.3	[15]
91	NbB_2	5	7256.313856	4.4	11	16.5	[15]
92	Nb_3B_2	0.05	6869.402054	4.36	21	22.46	[13]
93	NbB	0.05	7012.426853	4.375	8	21.53	[13]
94	Nb_3B_4	0.03	7116.057791	4.38571	27	22.46	[13]
95	TiB_2	0.01	7355.827511	4.41	10	36	[31]
96	TiB_2	0.03	7355.827511	4.41	10	33.05	[18]

97	TiB_2	0.05	7355.827511	4.41	10	33.34	[32]
98	TiB_2	0.2	7355.827511	4.41	10	32.44	[33]
99	TiB_2	0.5	7355.827511	4.41	10	25.5	[15]
100	TiB_2	5	7355.827511	4.41	10	19.2	[34]
101	TiB_2	5	7355.827511	4.41	10	19.7	[33]
102	TiB_2	10	7355.827511	4.41	10	20.3	[33]
103	TiB	0.03	7157.924635	4.39	7	27.46	[27]
104	CrB_2	0.05	7941.512183	4.46667	12	23.1	[35]
105	CrB_2	0.1	7941.512183	4.46667	12	20.5	[35]
106	CrB_2	0.2	7941.512183	4.46667	12	16.6	[35]
107	CrB_2	0.3	7941.512183	4.46667	12	16	[35]
108	CrB_2	0.5	7941.512183	4.46667	12	15.8	[35]
109	CrB_4	0.05	7870.62376	4.46	18	44	[35]
110	CrB_4	0.1	7870.62376	4.46	18	36.7	[35]
111	CrB_4	0.2	7870.62376	4.46	18	32.3	[35]
112	CrB_4	0.3	7870.62376	4.46	18	30.2	[35]
113	CrB_4	0.5	7870.62376	4.46	18	28.6	[35]
114	CrB	1	8030.789415	4.475	9	19.6	[36]
115	Cr_4B	0.05	8193.662024	4.49	27	12.16	[13]
116	Cr_2B	0.05	8120.901452	4.48333	15	13.24	[13]
117	Cr_3B_4	0.1	7992.425885	4.47143	30	14.71	[13]
118	Cr_5B_3	0.05	8098.321947	4.48125	39	14.91	[37]
119	WB	0.05	8303.765625	4.5	9	36.28	[18]
120	WB	0.5	8303.765625	4.5	9	28.2	[38]
121	WB_2	0.05	8120.901452	4.48333	12	42.2	[39]
122	WB_2	0.05	8120.901452	4.48333	12	43.9	[40]
123	WB_2	0.1	8120.901452	4.48333	12	29.6	[40]
124	WB_2	0.1	8120.901452	4.48333	12	33.8	[39]

125	WB_2	0.2	8120.901452	4.48333	12	27.1	[40]
126	WB_2	0.3	8120.901452	4.48333	12	26.4	[40]
127	WB_2	0.5	8120.901452	4.48333	12	25.5	[40]
128	WB_2	2	8120.901452	4.48333	12	22.9	[41]
129	WB_2	3	8120.901452	4.48333	12	22.2	[41]
130	WB_2	5	8120.901452	4.48333	12	22	[41]
131	WB_3	0.01	8030.789415	4.475	15	42	[42]
132	WB_3	0.025	8030.789415	4.475	15	31.8	[42]
133	WB_3	0.05	8030.789415	4.475	15	29.8	[42]
134	WB_3	0.1	8030.789415	4.475	15	27.9	[42]
135	WB_3	0.2	8030.789415	4.475	15	26.5	[42]
136	WB_3	0.3	8030.789415	4.475	15	26.2	[42]
137	WB_3	0.5	8030.789415	4.475	15	25.5	[42]
138	WB_4	0.05	7977.101882	4.47	18	38.64	[43]
139	WB_4	0.05	7977.101882	4.47	18	39.23	[44]
140	WB_4	0.05	7977.101882	4.47	18	43	[45]
141	WB_4	0.05	7977.101882	4.47	18	46.2	[46]
142	WB_4	0.2	7977.101882	4.47	18	32	[39]
143	WB_4	0.3	7977.101882	4.47	18	29.2	[39]
144	WB_4	0.5	7977.101882	4.47	18	25.4	[39]
145	WB_4	1	7977.101882	4.47	18	21.2	[39]
146	W_2B	0.05	8490.048399	4.51667	15	23.73	[18]
147	W_2B_5	0.05	8080.12287	4.47957	27	25.3	[47]
148	W_2B_5	0.03	8080.12287	4.47957	27	26.12	[27]
149	MoB_2	0.3	8303.765625	4.5	12	29.4	[41]
150	MoB_2	0.5	8303.765625	4.5	12	27.4	[41]
151	MoB_2	1	8303.765625	4.5	12	25.1	[41]
152	MoB_2	2	8303.765625	4.5	12	22.1	[41]

153	MoB_2	3	8303.765625	4.5	12	21.2	[41]
154	MoB_2	5	8303.765625	4.5	12	21	[41]
155	Mo_2B	0.05	8872.957063	4.55	15	24.52	[13]
156	MoB	0.05	8584.430744	4.525	9	23.04	[13]
157	MoB	0.05	8584.430744	4.525	9	24.52	[13]
158	OsB_2	0.025	9189.62084	4.57667	14	37	[48]
159	OsB_2	0.05	9189.62084	4.57667	14	23.5	[46]
160	OsB_2	0.075	9189.62084	4.57667	14	21.6	[48]
161	OsB_2	0.2	9189.62084	4.57667	14	17.8	[48]
162	OsB	0.05	9979.479338	4.64	11	14.4	[46]
163	Os_2B_3	0.05	9499.039333	4.602	25	21.8	[46]
164	VB_2	2	7256.313856	4.4	11	27.2	[49]
165	VB_2	0.05	7256.313856	4.4	11	45	[49]
166	ReB_2	0.05	8756.592045	4.54	13	39.3	[46]
167	ReB_2	0.05	8756.592045	4.54	13	38	[25]
168	ReB_2	0.05	8756.592045	4.54	13	48	[50]
169	ReB_2	0.05	8756.592045	4.54	13	40.5	[51]
170	ReB_2	0.05	8756.592045	4.54	13	48	[50]
171	ReB_2	0.075	8756.592045	4.54	13	37	[48]
172	ReB_2	0.1	8756.592045	4.54	13	29.8	[50]
173	ReB_2	0.2	8756.592045	4.54	13	30.8	[50]
174	RuB	0.05	9229.812275	4.58	11	13.6	[46]
175	RuB_2	0.025	8718.125921	4.53667	14	24.2	[52]
176	RuB_2	0.05	8718.125921	4.53667	14	19.9	[46]
177	RuB_2	0.05	8718.125921	4.53667	14	20.6	[52]
178	RuB_2	0.075	8718.125921	4.53667	14	19.2	[48]
179	RuB_2	0.1	8718.125921	4.53667	14	16.74	[52]
180	RuB_2	0.2	8718.125921	4.53667	14	14.4	[52]

181	$Os_{0.5}W_{0.5}B_2$	0.05	2878.722629	3.7716667	13	40.4	[46]
182	$YReB_4$	0.05	6061.320523	4.27	22	34.25	[53]
183	$YCrB_4$	0.05	5755.655573	4.2333333	21	37.5	[53]
184	$YRe_{0.5}Cr_{0.5}B_4$	0.05	5906.840576	4.2516667	21.5	42.48	[53]
185	$Y_{0.5}Sc_{0.5}CrB_4$	0.05	6032.985615	4.2666667	21	42.02	[53]
186	$YScReB_6$	0.05	5683.522953	4.2244444	31	41.33	[53]
187	Y_2ReB_6	0.05	5334.057471	4.18	31	35.69	[53]
188	Sc_2ReB_6	0.05	6051.863258	4.2688889	31	34.74	[53]
189	Y_3ReB_7	0.05	4794.512246	4.1063636	37	34.31	[53]
190	Y_3ReB_7	0.1	4794.512246	4.1063636	37	30.93	[53]
191	Y_3ReB_7	0.2	4794.512246	4.1063636	37	27.37	[53]
192	Y_3ReB_7	0.3	4794.512246	4.1063636	37	24.8	[53]
193	Y_3ReB_7	0.5	4794.512246	4.1063636	37	21.35	[53]
194	Y_3WB_7	0.05	4794.512246	4.1063636	36	16.76	[53]
195	Y_3WB_7	0.1	4794.512246	4.1063636	36	14.12	[53]
196	Y_3WB_7	0.2	4794.512246	4.1063636	36	14.07	[53]
197	Y_3WB_7	0.3	4794.512246	4.1063636	36	13.39	[53]
198	Y_3WB_7	0.5	4794.512246	4.1063636	36	13.21	[53]
199	Y_3MoB_7	0.05	1178.420166	3.25	36	29.29	[53]
200	Y_3MoB_7	0.1	1178.420166	3.25	36	17.11	[53]
201	Y_3MoB_7	0.2	1178.420166	3.25	36	13.21	[53]
202	Y_3MoB_7	0.3	1178.420166	3.25	36	11.93	[53]
203	Y_3MoB_7	0.5	1178.420166	3.25	36	11.61	[53]
204	YMo_3B_7	0.05	6947.111047	4.3681818	42	26.78	[53]
205	YMo_3B_7	0.1	6947.111047	4.3681818	42	25.1	[53]
206	YMo_3B_7	0.2	6947.111047	4.3681818	42	22.36	[53]
207	YMo_3B_7	0.3	6947.111047	4.3681818	42	21.47	[53]
208	YMo_3B_7	0.5	6947.111047	4.3681818	42	21.1	[53]

209	$YMo_{2.8}W_{0.2}B_7$	0.05	6938.440706	4.3672727	42	34.37	[53]
210	$YMo_{2.8}W_{0.2}B_7$	0.1	6938.440706	4.3672727	42	28.78	[53]
211	$YMo_{2.8}W_{0.2}B_7$	0.2	6938.440706	4.3672727	42	24.23	[53]
212	$YMo_{2.8}W_{0.2}B_7$	0.3	6938.440706	4.3672727	42	22.45	[53]
213	$YMo_{2.8}W_{0.2}B_7$	0.5	6938.440706	4.3672727	42	22.5	[53]
214	ScB_{12}	0.05	7030.941502	4.376923077	39	41.29	[54]
215	CaB_6	0.03	5682.241752	4.224285714	20	26.48	[55]
216	BaB_6	0.03	5489.031744	4.2	20	29.42	[55]
217	SrB_6	0.03	5366.955444	4.184285714	20	28.54	[56]
218	ScB_2	0.2	4986.577607	4.1333333	9	17.46	[18]
219	ScB_{12}	0.05	7030.941502	4.3769231	39	41.7	[26]
220	YB_{12}	0.05	6739.544931	4.3461538	39	40.9	[26]
221	YB_{12}	0.05	6739.544931	4.3461538	39	45.11	[57]
222	V_3B_2	0.05	6869.402054	4.36	21	22.36	[13]
223	V_3B_4	0.05	7116.099517	4.3857142	27	23.05	[13]

Supplementary Note 2: Feature Selection

Table S2. 149 features based on Magpie data package and knowledge.

Elements attributes		
Feature	**Abbreviation**	**Description**
Atomic Number	min_Number	The minimum atomic number of all the elements in the composition
	max_Number	The maximum atomic number of all the elements in the composition
	maxdiff_Number0	The range of atomic number of all the elements in the composition
	mean_Number	The fraction-weighted mean of the atomic number for the composition.
	dev_Number	The average deviation of the atomic number for the composition.
	most_Number	The mode of the atomic number for the composition.
Mendeleev Number	min_MendeleevNumber	The minimum Mendeleev number of all the elements in the composition.
	max_MendeleevNumber	The maximum Mendeleev number of all the elements in the composition.

	maxdiff_MendeleevNumber	The range of Mendeleev numbers of all the elements in the composition.
	mean_MendeleevNumber	The fraction-weighted mean of the Mendeleev number for the composition.
	dev_MendeleevNumber	The average deviation of the Mendeleev number for the composition
	most_MendeleevNumber	The mode of the Mendeleev number for the composition.
Atomic Weight	min_AtomicWeight	The minimum atomic weight of all the elements in the composition.
	max_AtomicWeight	The maximum atomic weight of all the elements in the composition.
	maxdiff_AtomicWeight	The range of atomic weight of all the elements in the composition
	mean_AtomicWeight	The fraction-weighted mean of the atomic weight for the composition.
	dev_AtomicWeight	The average deviation of the atomic weight for the composition.
	most_AtomicWeight	The mode of the atomic weight for the composition.
Melting Temperature	min_MeltingT	The minimum melting temperature of all the elements in the composition.
	max_MeltingT	The maximum melting temperature of all the elements in the composition.
	maxdiff_MeltingT	The range of melting temperature of all the elements in the composition.
	mean_MeltingT	The fraction-weighted mean of the melting temperature for the composition.
	dev_MeltingT	The average deviation of the melting temperature for the composition.
	most_MeltingT	The mode of the melting temperature for the composition.
Column	min_Column	The minimum column of all the elements in the composition.
	max_Column	The maximum column of all the elements in the composition.
	maxdiff_Column	The range of column of all the elements in the composition.
	mean_Column	The fraction-weighted mean of the column for the composition.
	dev_Column	The average deviation of the column for the composition.
	most_Column	The mode of the column for the composition.
Row	min_Row	The minimum row of all the elements in the composition.
	max_Row	The maximum row of all the elements in the composition.
	maxdiff_Row	The range of row of all the elements in the composition.
	mean_Row	The fraction-weighted mean of the row for the composition.
	dev_Row	The average deviation of the row for the composition.
	most_Row	The mode of the row for the composition.
Covalent Radius	min_CovalentRadius	The minimum covalent radius of all the elements in the composition.

	max_CovalentRadius	The maximum covalent radius of all the elements in the composition.
	maxdiff_CovalentRadius	The range of covalent radius of all the elements in the composition.
	mean_CovalentRadius	The fraction-weighted mean of the covalent radius for the composition.
	dev_CovalentRadius	The average deviation of the covalent radius for the composition.
	most_CovalentRadius	The mode of the covalent radius for the composition.
Electronegativity	min_Electronegativity	The minimum electronegativity of all the elements in the composition.
	max_Electronegativity	The maximum electronegativity of all the elements in the composition.
	maxdiff_Electronegativity	The range of electronegativity of all the elements in the composition.
	mean_Electronegativity	The fraction-weighted mean of the electronegativity for the composition.
	dev_Electronegativity	The average deviation of the electronegativity for the composition.
	most_Electronegativity	The mode of the electronegativity for the composition.
s Valence Electrons	min_NsValence	The minimum s-valence electrons of all the elements in the composition.
	max_NsValence	The maximum s-valence electrons of all the elements in the composition.
	maxdiff_NsValence	The range of s-valence electrons of all the elements in the composition.
	mean_NsValence	The fraction-weighted mean of the s-valence electrons for the composition.
	dev_NsValence	The average deviation of the s-valence electrons for the composition.
	most_NsValence	The mode of the s-valence electrons for the composition.
p Valence Electrons	min_NpValence	The minimum p-valence electrons of all the elements in the composition.
	max_NpValence	The maximum p-valence electrons of all the elements in the composition.
	maxdiff_NpValence	The range of p-valence electrons of all the elements in the composition.
	mean_NpValence	The fraction-weighted mean of the p-valence electrons for the composition.
	dev_NpValence	The average deviation of the p-valence electrons for the composition.
	most_NpValence	The mode of the p-valence electrons for the composition.
d Valence Electrons	min_NdValence	The minimum d-valence electrons of all the elements in the composition.
	max_NdValence	The maximum d-valence electrons of all the elements in the composition.
	maxdiff_NdValence	The range of d-valence electrons of all the elements in the composition.
	mean_NdValence	The fraction-weighted mean of the d-valence electrons for the composition.
	dev_NdValence	The average deviation of the d-valence electrons for the composition.
	most_NdValence	The mode of the d-valence electrons for the composition.

f Valence Electrons	min_NfValence	The minimum f-valence electrons of all the elements in the composition.
	max_NfValence	The maximum f-valence electrons of all the elements in the composition.
	maxdiff_NfValence	The range of f-valence electrons of all the elements in the composition.
	mean_NfValence	The fraction-weighted mean of the f-valence electrons for the composition.
	dev_NfValence	The average deviation of the f-valence electrons for the composition.
	most_NfValence	The mode of the f-valence electrons for the composition.
Total Valance Electrons	min_NValence	The minimum total valence electrons of all the elements in the composition.
	max_NValence	The maximum total valence electrons of all the elements in the composition.
	maxdiff_NValence	The range of total valence electrons of all the elements in the composition.
	mean_NValence	The fraction-weighted mean of the total valence electrons for the composition.
	dev_NValence	The average deviation of the total valence electrons for the composition.
	most_NValence	The mode of the total valence electrons for the composition.
Unfilled s States	min_NsUnfilled	The minimum unfilled s-valence electrons of all the elements in the composition.
	max_NsUnfilled	The maximum unfilled s-valence electrons of all the elements in the composition.
	maxdiff_NsUnfilled	The range of unfilled s-valence electrons of all the elements in the composition.
	mean_NsUnfilled	The fraction-weighted mean of the unfilled s-valence electrons for the composition.
	dev_NsUnfilled	The average deviation of the unfilled s-valence electrons for the composition.
	most_NsUnfilled	The mode of the unfilled s-valence electrons for the composition
Unfilled p States	min_NpUnfilled	The minimum unfilled p-valence electrons of all the elements in the composition.
	max_NpUnfilled	The maximum unfilled p-valence electrons of all the elements in the composition.
	maxdiff_NpUnfilled	The range of unfilled p-valence electrons of all the elements in the composition.
	mean_NpUnfilled	The fraction-weighted mean of the unfilled p-valence electrons for the composition.
	dev_NpUnfilled	The average deviation of the unfilled p-valence electrons for the composition.

	most_NpUnfilled	The mode of the unfilled p-valence electrons for the composition.
Unfilled d States	min_NdUnfilled	The minimum unfilled d-valence electrons of all the elements in the composition.
	max_NdUnfilled	The maximum unfilled d-valence electrons of all the elements in the composition.
	maxdiff_NdUnfilled	The range of unfilled d-valence electrons of all the elements in the composition.
	mean_NdUnfilled	The fraction-weighted mean of the unfilled d-valence electrons for the composition.
	dev_NdUnfilled	The average deviation of the unfilled d-valence electrons for the composition.
	most_NdUnfilled	The mode of the unfilled d-valence electrons for the composition.
Unfilled f States	min_NfUnfilled	The minimum unfilled f-valence electrons of all the elements in the composition.
	max_NfUnfilled	The maximum unfilled f-valence electrons of all the elements in the composition.
	maxdiff_NfUnfilled	The range of unfilled f-valence electrons of all the elements in the composition
	mean_NfUnfilled	The fraction-weighted mean of the unfilled f-valence electrons for the composition.
	dev_NfUnfilled	The average deviation of the unfilled f-valence electrons for the composition.
	most_NfUnfilled	The mode of the unfilled f-valence electrons for the composition.
Total Unfilled States	min_NUnfilled	The minimum unfilled total valence electrons of all the elements in the composition.
	max_NUnfilled	The maximum unfilled total valence electrons of all the elements in the composition.
	maxdiff_NUnfilled	The range of unfilled total valence electrons of all the elements in the composition.
	mean_NUnfilled	The fraction-weighted mean of the unfilled total valence electrons for the composition.
	dev_NUnfilled	The average deviation of the unfilled total valence electrons for the composition.
	most_NUnfilled	The mode of the unfilled total valence electrons for the composition.
	min_GSvolume_pa	The minimum specific volume of all the elements in the composition.
	max_GSvolume_pa	The maximum specific volume of all the elements in the composition.

Specific Volume of 0 K Ground State	maxdiff_GSvolume_pa	The range of the specific volume of all the elements in the composition.
	mean_GSvolume_pa	The fraction-weighted mean of the specific volume for the composition.
	dev_GSvolume_pa	The average deviation of the specific volume for the composition.
	most_GSvolume_pa	The mode of the specific volume for the composition.
Band Gap Energy of 0 K Ground State	min_GSbandgap	The minimum band gap energy of all the elements in the composition
	max_GSbandgap	The maximum band gap energy of all the elements in the composition
	maxdiff_GSbandgap	The range of band gap energy of all the elements in the composition
	mean_GSbandgap	The fraction-weighted mean of the band gap energy for the composition.
	dev_GSbandgap	The average deviation of the band gap energy for the composition.
	most_GSbandgap	The mode of the band gap energy for the composition.
Magnetic Moment (per atom) of 0 K ground state	min_GSmagmom	The minimum magnetic moment of all the elements in the composition
	max_GSmagmom	The maximum magnetic moment of all the elements in the composition
	maxdiff_GSmagmom	The range of magnetic moment of all the elements in the composition
	mean_GSmagmom	The fraction-weighted mean of the magnetic moment for the composition.
	dev_GSmagmom	The average deviation of the magnetic moment for the composition.
	most_GSmagmom	The mode of the magnetic moment for the composition.
Space Group Number of 0 K Ground State	min_SpaceGroupNumber	The minimum space group number of all the elements in the composition
	max_SpaceGroupNumber	The maximum space group number of all the elements in the composition
	maxdiff_SpaceGroupNumber	The range of space group number of all the elements in the composition
	mean_SpaceGroupNumber	The fraction-weighted mean of the space group number for the composition.
	dev_SpaceGroupNumber	The average deviation of the space group number for the composition.
	most_SpaceGroupNumber	The mode of the space group number for the composition.
Electronic structure Attributes		
avg s valence electrons	frac_sValence	The avg s valence electrons of the space group number for the composition.
avg p valence electrons	frac_pValence	The avg p valence electrons of the space group number for the composition.
avg d valence electrons	frac_dValence	The avg d valence electrons of the space group number for the composition.

avg f valence electrons	frac_fValence	The avg f valence electrons of the space group number for the composition.
Ionic compound Attributes		
Boolean denoting	CanFormIonic	The candidate to form the neutral ionic compound.
Ionic Character	MaxIonicChar	The max ionic character between any two constituent elements.
	MeanIonicChar	The mean ionic character for the composition.
Stoichiometricv Attributes		
NComp	NComp	The types of elements contained in borides.
Comp_L2Norm	Comp_L2Norm	The fraction of elements present without regard to what the elements are. All are based on L^P norms with varying p values to capture various degrees of change.(P=2)
Comp_L3Norm	Comp_L3Norm	The fraction of elements present without regard to what the elements are. All are based on L^P norms with varying p values to capture various degrees of change.(P=3)
Comp_L5Norm	Comp_L5Norm	The fraction of elements present without regard to what the elements are. All are based on L^P norms with varying p values to capture various degrees of change.(P=5)
Comp_L7Norm	Comp_L7Norm	The fraction of elements present without regard to what the elements are. All are based on L^P norms with varying p values to capture various degrees of change.(P=7)
Expert knowledge Attributes		
Load	load	The load applied to measure boride Vickers hardness.
Electron-Work Function	EWF	The electron-work function of boride ceramics.
	EWF^6	The six power for electron-work function of boride ceramics.
Valence electrons Concentration	VEC	The valence electrons concentration for the borides.
……	……	……

Correlation screening

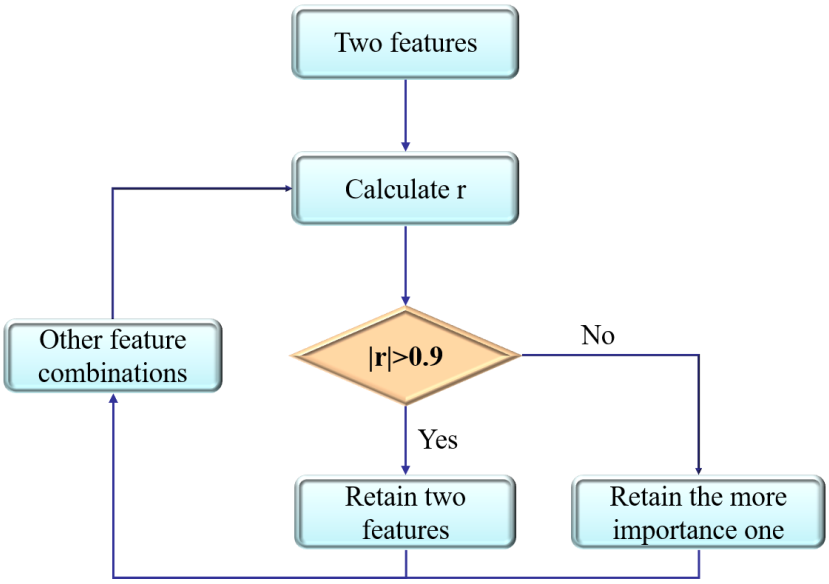

Figure S2. Workflow for correlation screening. Where the pearson correlation coefficient (PCC, r), $r(\hat{Y},Y)=\frac{Cov(\hat{Y},Y)}{\sqrt{Var[\hat{Y}]Var[Y]}}$

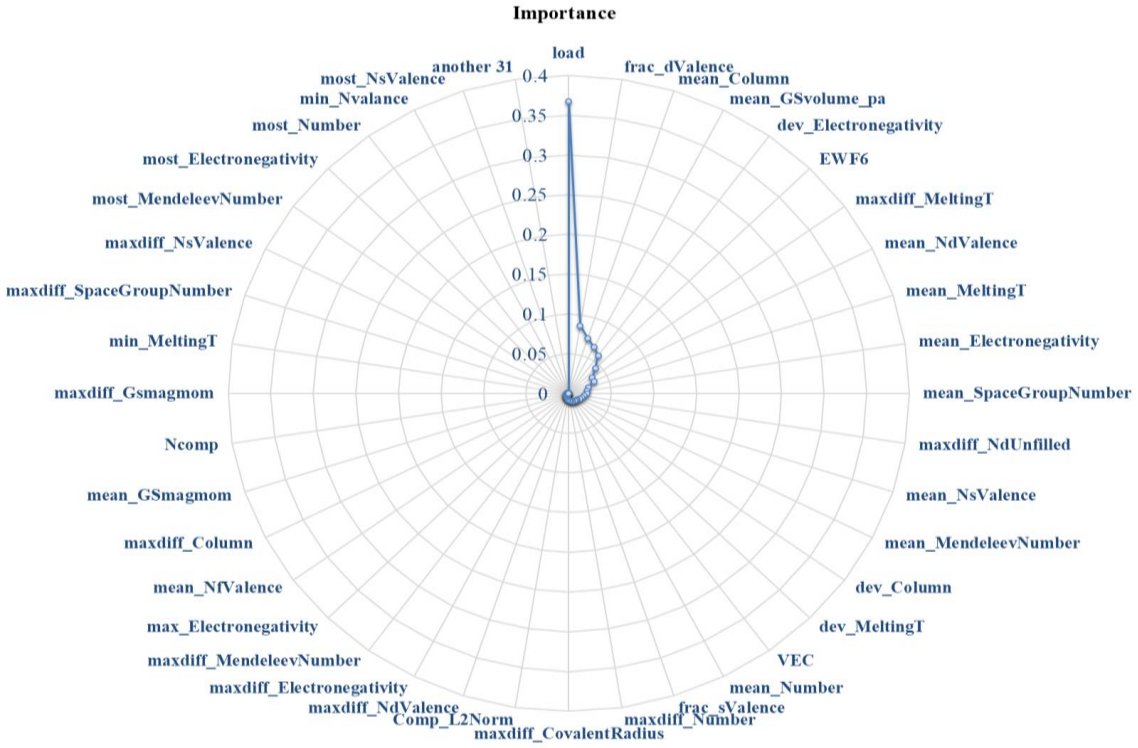

Figure S3. The importance of 70 featutres after colleration screening.

Table S3. The importance of 70 featutres after colleration screening.

Index	Feature	Importance
1	load	0.367551
2	frac_dValence	0.08625
3	mean_Column	0.072564
4	mean_GSvolume_pa	0.06569
5	dev_Electronegativity	0.058798
6	EWF6	0.044429
7	maxdiff_MeltingT	0.033848
8	mean_NdValence	0.033488
9	mean_MeltingT	0.024683
10	mean_Electronegativity	0.021383
11	mean_SpaceGroupNumber	0.021322
12	maxdiff_NdUnfilled	0.018391
13	mean_NsValence	0.016413
14	mean_MendeleevNumber	0.014947
15	dev_Column	0.012558
16	dev_MeltingT	0.012266
17	VEC	0.012048
18	mean_Number	0.011171
19	frac_sValence	0.010191
20	maxdiff_Number	0.009553
21	maxdiff_CovalentRadius	0.008047
22	Comp_L2Norm	0.007444
23	maxdiff_NdValence	0.005796
24	maxdiff_Electronegativity	0.005151
25	maxdiff_MendeleevNumber	0.005053
26	max_Electronegativity	0.00341

27	mean_NfValence	0.002932
28	maxdiff_Column	0.002785
29	mean_GSmagmom	0.002689
30	Ncomp	0.002099
31	maxdiff_Gsmagmom	0.001892
32	min_MeltingT	0.00165
33	maxdiff_SpaceGroupNumber	0.001505
34	maxdiff_NsValence	0.001096
35	most_MendeleevNumber	0.000408
36	most_Electronegativity	0.00036
37	most_Number	0.000106
38	min_Nvalance	0.000089
39	most_NsValence	0.000012
40	Another 31	0

Random forest

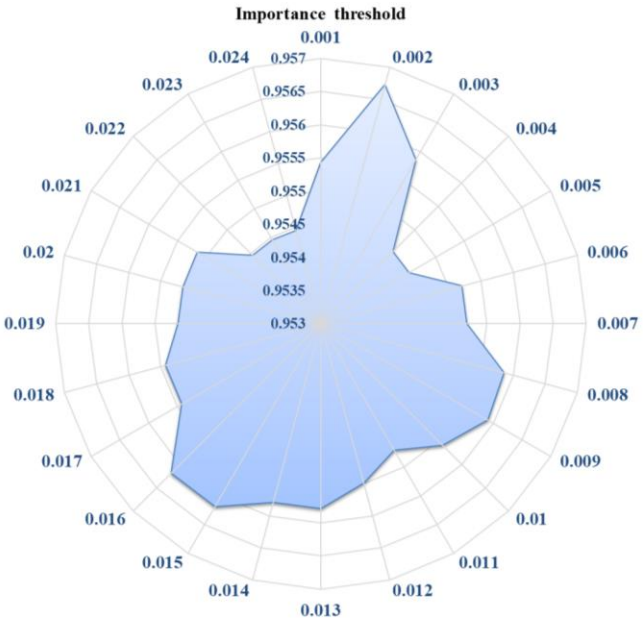

Figure S4. RF algorithm for feature screening.

Table S4. Feature Abbreviation of F1-F3.

Number	Abbreviation	Number	Abbreviation
F1	load	**F16**	maxdiff_CovalentRadius
F2	EWF[6]	**F17**	mean_Electronegativity
F3	VEC	**F18**	maxdiff_Electronegativity
F4	NComp	**F19**	dev_Electronegativity
F5	Comp_L2Norm	**F20**	max_Electronegativity
F6	mean_Number	**F21**	mean_NsValence
F7	maxdiff_Number	**F22**	mean_NdValence
F8	mean_MendeleevNumber	**F23**	maxdiff_NdValence
F9	maxdiff_MendeleevNumber	**F24**	mean_NfValence
F10	mean_MeltingT	**F25**	maxdiff_NdUnfilled
F11	maxdiff_MeltingT	**F26**	mean_GSvolume_pa
F12	dev_MeltingT	**F27**	mean_GSmagmom
F13	mean_Column	**F28**	mean_SpaceGroupNumber
F14	maxdiff_Column	**F29**	frac_sValence
F15	dev_Column	**F30**	frac_dValence

Forward selection

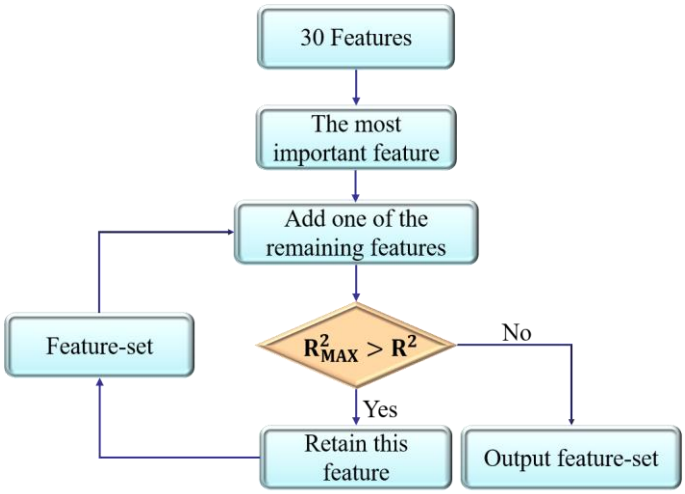

Figure S5. Workflow for forward selection.

Best-subset selection :

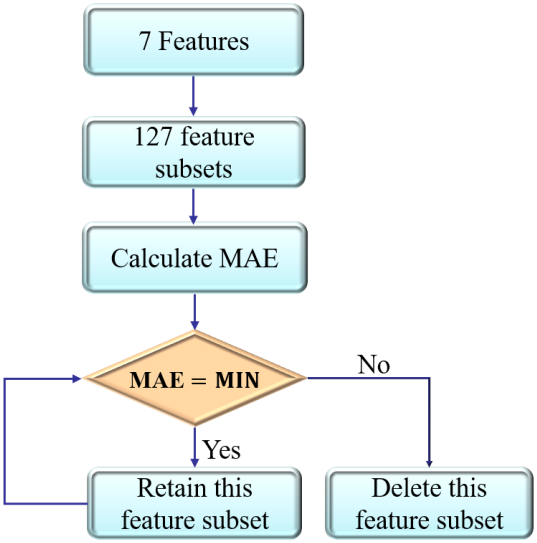

Figure S6. Workflow for best-subset selection.

Supplementary Note 3: Algorithm selection

The R-Square (R^2) and Mean Absolute Error (MAE) were used as model evaluation scale.

$$R^2=1-\frac{\sum_i(\hat{y}_i-y_i)^2}{\sum_i(\bar{y}_i-y_i)^2} \quad (1)$$

$$MAE=\frac{1}{m}\sum_{i=1}^{m}|(y_i-\hat{y}_i)| \quad (2)$$

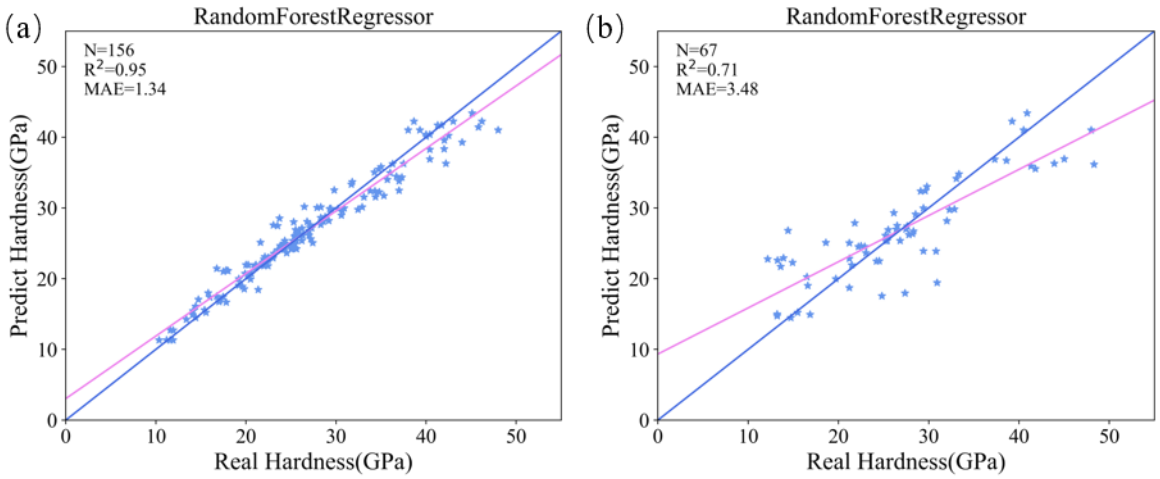

Figure S7. the predicted hardness as a function of the real hardness of the RF model for (a) the training set, (b) the testing set (N represents the number of the sample).

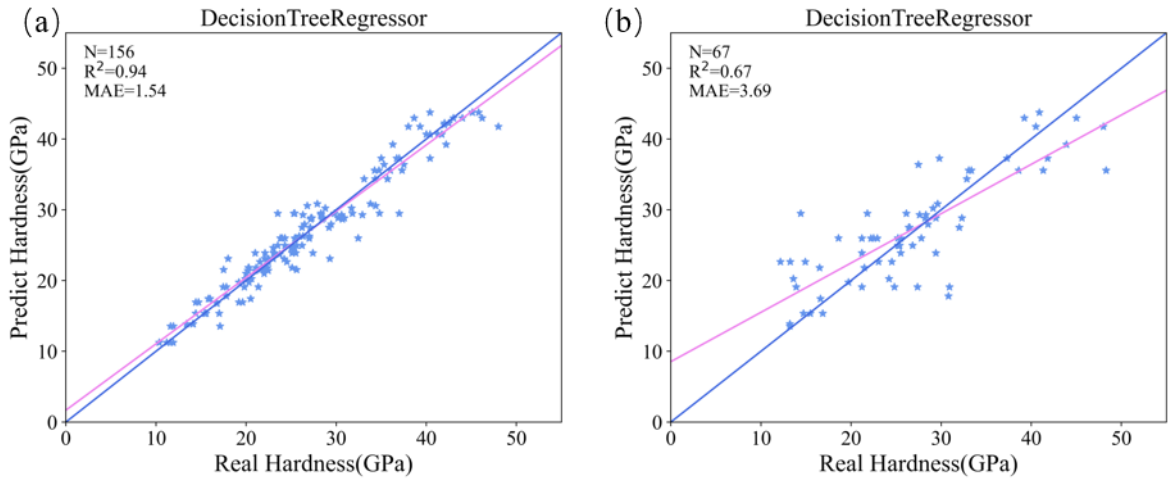

Figure S8. the predicted hardness as a function of the real hardness of the DT model for (a) the training set, (b) the testing set .

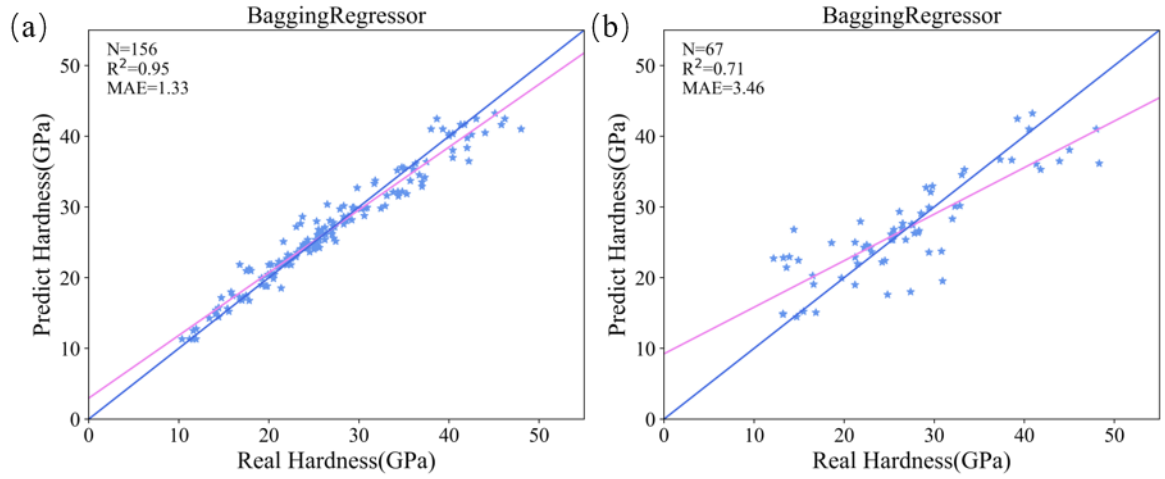

Figure S9. the predicted hardness as a function of the real hardness of the Bagging model for (a) the training set, (b) the testing set

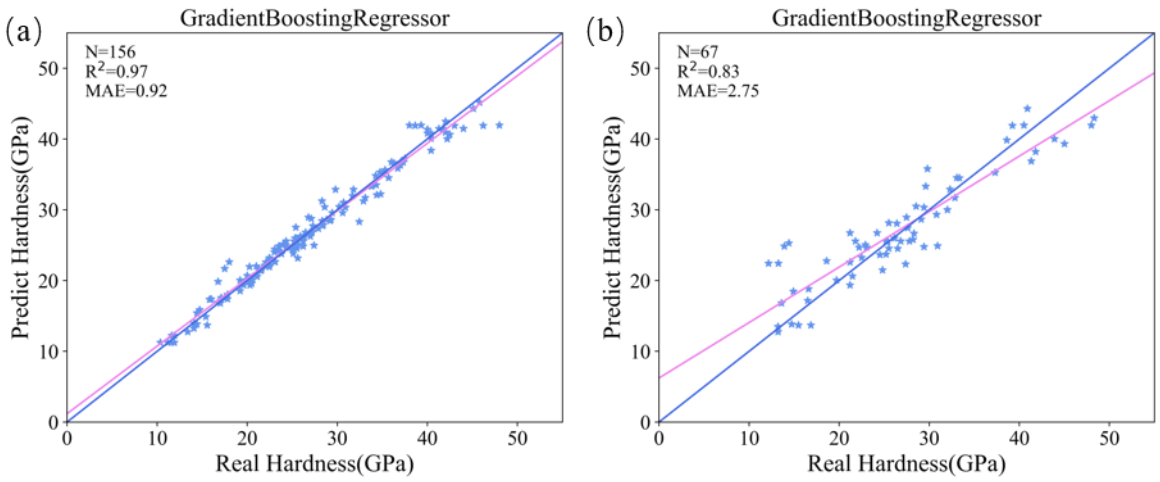

Figure S10. the predicted hardness as a function of the real hardness of the GBRT model for (a) the training set, (b) the testing set .

Supplementary Note 4: Knowledge-based modeling

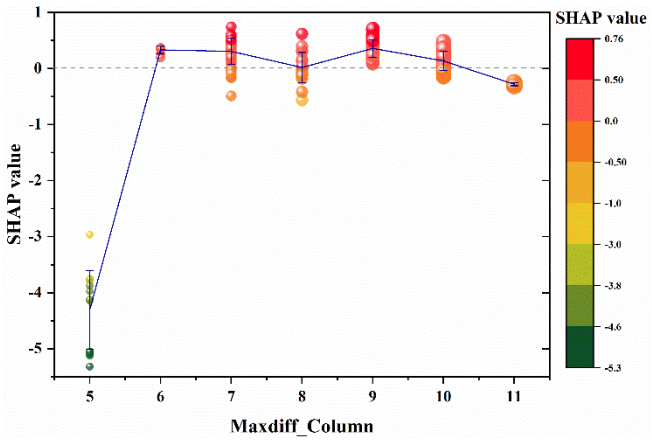

Figure S11. The SHAP value changes with the Maxdiff_Column

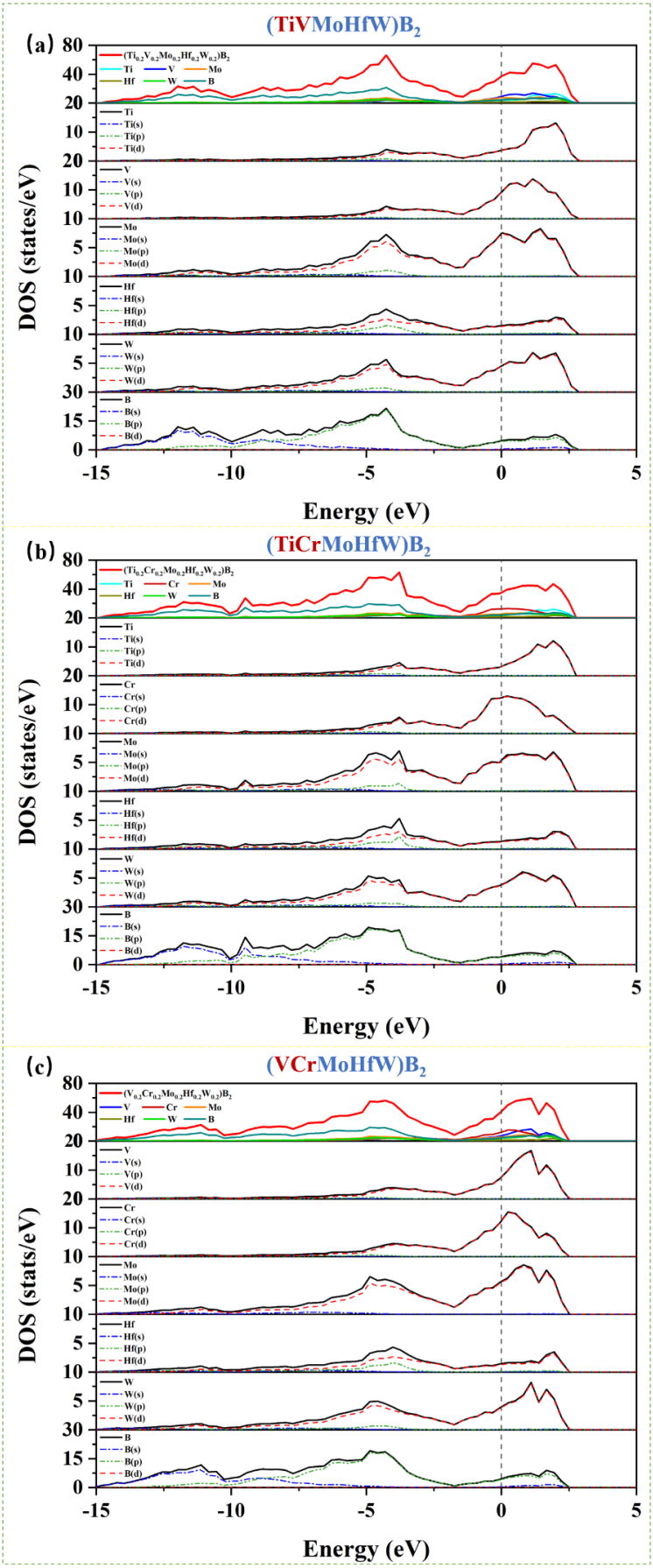

Figure S12. TDOS and PDOS of: (a) $(TiVMoHfW)B_2$, (b) $(TiCrMoHfW)B_2$, (c) $(VCrMoHfW)B_2$.

Supplementary Note 5: Validation

Table S5. Model performance on candidate compositions ($Hv_{0.2}$).

Index	Compositiobns	EWF[6]	frac_dValence	mean_Electronegativity	maxdiff_Column	Hardness (GPa)
1	$TiCrMoHfWB_2$	7510.62250	0.30000	1.87143	9	33.35313
2	$TiVMoTaWB_2$	7613.03079	0.28333	1.89571	9	32.49396
3	$VNbMoHfWB_2$	7355.82751	0.30000	1.87571	9	32.34938
4	$VCrMoHfWB_2$	7490.27924	0.31148	1.88429	9	32.34235
5	$TiNbMoTaWB_2$	7613.03079	0.30000	1.89143	9	32.28824
6	$TiCrMoTaWB_2$	7751.38298	0.31148	1.90000	9	31.95944
7	$VNbMoTaWB_2$	7592.45659	0.31148	1.90429	8	31.80608
8	$VZrMoTaWB_2$	7422.79970	0.28333	1.86571	9	31.56106
9	$CrZrMoTaWB_2$	7558.26922	0.31148	1.87000	9	31.56102
10	$ZrNbMoTaWB_2$	7422.79970	0.30000	1.86143	9	30.97503
11	$TiNbMoHfWB_2$	7375.86608	0.28814	1.86286	9	30.97133
12	$TiZrMoTaWB_2$	7442.99015	0.27119	1.85286	9	30.92132
13	$TiVMoHfWB_2$	7375.86608	0.27119	1.86714	9	30.51141
14	$TiMoHfTaWB_2$	7342.49369	0.21918	1.84857	9	30.44725
15	$CrMoHfTaWB_2$	7456.47586	0.25333	1.86571	9	29.52559
16	$VMoHfTaWB_2$	7322.53072	0.22973	1.86143	9	28.93763
17	$NbMoHfTaWB_2$	7322.53072	0.24324	1.85714	9	28.83760
18	$TiVZrMoWB_2$	7476.74260	0.35556	1.87143	9	27.27869
19	$CrNbMoHfWB_2$	7490.27924	0.32787	1.88000	9	26.38757
20	$CrZrMoHfWB_2$	7322.53072	0.30000	1.84143	9	26.36299
21	$TiZrHfTaWB_2$	6983.62514	0.18310	1.73000	9	25.76605
22	$TiVCrTaWB_2$	7544.63025	0.28333	1.82429	9	24.88154
23	$TiCrNbTaWB_2$	7544.63025	0.30000	1.82000	9	24.86009
24	$VCrMoTaWB_2$	7730.49759	0.32258	1.91286	8	24.57907

25	$CrNbMoTaWB_2$	7730.49759	0.33871	1.90857	8	24.43529
26	$TiZrNbMoWB_2$	7476.74260	0.37778	1.86714	9	24.28559
27	$TiVNbTaWB_2$	7409.36477	0.27119	1.81571	9	24.26580
28	$VCrNbTaWB_2$	7524.21024	0.31148	1.83286	8	24.14317
29	$TiCrNbHfWB_2$	7309.24723	0.28814	1.79143	9	24.10443
30	$TiCrMoHfTaB_2$	7309.24723	0.28814	1.74857	9	24.10443
31	$VCrZrTaWB_2$	7355.82751	0.28333	1.79429	9	24.10443
32	$CrZrNbTaWB_2$	7355.82751	0.30000	1.79000	9	24.10443
33	$VCrNbHfWB_2$	7289.35963	0.30000	1.80429	9	23.97181
34	$TiVCrHfWB_2$	7309.24723	0.27119	1.79571	9	23.43858
35	$TiCrZrTaWB_2$	7375.86608	0.27119	1.78143	9	23.43858
36	$VZrNbMoWB_2$	7456.47586	0.39130	1.88000	9	23.15619
37	$TiCrZrMoWB_2$	7613.03079	0.39130	1.87571	9	23.13669
38	$VCrMoHfTaB_2$	7289.35963	0.30000	1.76143	9	23.09296
39	$ZrNbHfTaWB_2$	6964.47882	0.20833	1.73857	9	22.94971
40	$VZrHfTaWB_2$	6964.47882	0.19444	1.74286	9	22.71792
41	$CrNbMoHfTaB_2$	7289.35963	0.31667	1.75714	9	22.66463
42	$TiZrMoHfWB_2$	$721_{0.2}5958$	0.25862	1.82429	9	22.48415
43	$CrZrNbMoWB_2$	7592.45659	0.42553	1.88429	9	22.14510
44	$VCrZrMoWB_2$	7592.45659	0.40426	1.88857	9	22.09304
45	$TiVCrZrWB_2$	7409.36477	0.35556	1.80000	9	22.08178
46	$TiZrNbTaWB_2$	7243.13055	0.25862	1.77286	9	21.98366
47	$TiVNbMoWB_2$	7647.42437	0.39130	1.91000	9	21.92565
48	$TiCrHfTaWB_2$	7276.12631	0.21918	1.77714	9	21.76183
49	$ZrNbMoHfWB_2$	7190.59674	0.28814	1.83286	9	21.74918
50	$VZrNbTaWB_2$	7223.39302	0.27119	1.78571	9	21.73245
51	$TiCrZrHfTaB_2$	6951.73892	0.24561	1.63000	9	21.70347
52	$TiVNbHfTaB_2$	6983.62514	0.24561	1.66429	9	21.66476

53	$TiVZrNbHfB_2$	6856.80728	0.30952	1.64000	9	21.58951
54	$VZrMoHfWB_2$	7190.59674	0.27119	1.83714	9	21.51652
55	$VCrHfTaWB_2$	7256.31386	0.22973	1.79000	9	21.40315
56	$TiVZrTaWB_2$	7243.13055	0.24138	1.77714	9	21.38650
57	$CrNbHfTaWB_2$	7256.31386	0.24324	1.78571	9	21.38650
58	$CrZrNbHfTaB_2$	6932.66549	0.27586	1.63857	9	21.36423
59	$TiVCrMoWB_2$	7786.29644	0.40426	1.91857	9	20.94215
60	$TiCrNbMoWB_2$	7786.29644	0.42553	1.91429	9	20.94215
61	$TiVZrNbWB_2$	7276.12631	0.34091	1.79143	9	20.92283
62	$TiVZrMoTaB_2$	7276.12631	0.34091	1.74857	9	20.92283
63	$VNbMoHfTaB_2$	7157.92464	0.28814	1.75286	9	20.91364
64	$TiVCrZrHfB_2$	6983.62514	0.32558	1.64857	9	20.86552
65	$VCrZrHfTaB_2$	6932.66549	0.25862	1.64286	9	20.86188
66	$TiCrZrNbHfB_2$	6983.62514	0.34884	1.64429	9	20.85629
67	$CrZrNbHfWB_2$	7125.37634	0.28814	1.76143	9	20.82726
68	$CrZrMoHfTaB_2$	7125.37634	0.28814	1.71857	9	20.82726
69	$TiNbHfTaWB_2$	7144.89048	0.20833	1.76857	9	20.74423
70	$TiNbMoHfTaB_2$	7177.51301	0.27586	1.74000	9	20.66616
71	$VCrNbHfTaB_2$	7092.95147	0.28814	1.68143	9	20.62641
72	$VCrNbMoWB_2$	7765.33267	0.43750	1.92714	8	20.60247
73	$TiCrNbHfTaB_2$	7112.39160	0.27586	1.66857	9	20.56919
74	$TiVCrNbWB_2$	7578.76621	0.39130	1.83857	9	20.52010
75	$ZrMoHfTaWB_2$	7157.92464	0.21918	1.81857	9	20.46600
76	$TiVHfTaWB_2$	7144.89048	0.19444	1.77286	9	20.44468
77	$TiVCrZrTaB_2$	$721_{0.2}5958$	0.34091	1.67714	9	20.40210
78	$ZrNbMoHfTaB_2$	6996.41371	0.27586	1.71000	9	20.39193
79	$TiVZrHfTaB_2$	6825.40451	0.21429	1.62571	9	20.27537
80	$TiZrNbHfTaB_2$	6825.40451	0.23214	1.62143	9	20.19445

81	$VZrNbHfTaB_2$	6806.62044	0.24561	1.63429	9	20.19445
82	$TiVNbHfWB_2$	7177.51301	0.25862	1.78714	9	20.16380
83	$TiVMoHfTaB_2$	7177.51301	0.25862	1.74429	9	20.16380
84	$VCrZrHfWB_2$	7125.37634	0.27119	1.76571	9	20.15715
85	$TiCrZrHfWB_2$	7144.89048	0.25862	1.75286	9	20.09570
86	$TiVCrHfTaB_2$	7112.39160	0.25862	1.67286	9	20.06683
87	$VCrZrNbWB_2$	7389.25038	0.39130	1.80857	9	20.03355
88	$TiVCrNbTaB_2$	7375.86608	0.37778	1.71571	9	20.03158
89	$TiVCrMoHfB_2$	7342.49369	0.37778	1.76714	9	20.03158
90	$TiVNbMoTaB_2$	7442.99015	0.37778	1.78714	9	20.03158
91	$TiCrZrNbWB_2$	7409.36477	0.37778	1.79571	9	20.03158
92	$TiCrZrMoTaB_2$	7409.36477	0.37778	1.75286	9	20.03158
93	$VCrZrMoTaB_2$	7389.25038	0.39130	1.76571	9	19.92578
94	$TiVCrMoTaB_2$	7578.76621	0.39130	1.79571	9	19.90628
95	$VZrNbHfWB_2$	6996.41371	0.25862	1.75714	9	19.88958
96	$VZrMoHfTaB_2$	6996.41371	0.25862	1.71429	9	19.88958
97	$TiZrNbMoTaB_2$	7276.12631	0.36364	1.74429	9	19.84936
98	$VCrZrNbHfB_2$	6964.47882	0.36364	1.65714	9	19.84671
99	$VNbHfTaWB_2$	7125.37634	0.21918	1.78143	9	19.55527
100	$TiCrNbMoHfB_2$	7342.49369	0.40000	1.76286	9	19.48941
101	$VCrNbMoHfB_2$	7322.53072	0.41304	1.77571	9	19.48941
102	$CrZrNbMoTaB_2$	7389.25038	0.41304	1.76143	9	19.48941
103	$TiCrNbMoTaB_2$	7578.76621	0.41304	1.79143	9	19.46991
104	$TiVZrHfWB_2$	7015.63314	0.22807	1.74857	9	19.46878
105	$TiZrNbHfWB_2$	7015.63314	0.24561	1.74429	9	19.38787
106	$TiZrMoHfTaB_2$	7015.63314	0.24561	1.70143	9	19.38787
107	$CrZrHfTaWB_2$	7092.95147	0.21918	1.74714	9	19.35442
108	$TiVNbMoHfB_2$	7210.25958	0.36364	1.75857	9	19.32863

109	$TiCrZrNbTaB_2$	7210.25958	0.36364	1.67286	9	19.32863
110	$TiZrNbMoHfB_2$	7047.76331	0.34884	1.71571	9	18.75485
111	$TiVZrMoHfB_2$	7047.76331	0.32558	1.72000	9	18.74983
112	$TiVZrNbTaB_2$	7080.01600	0.32558	1.66857	9	18.69944
113	$VZrNbMoTaB_2$	7256.31386	0.37778	1.75714	9	18.63984
114	$VCrNbMoTaB_2$	7558.26922	0.42553	1.80429	8	18.55614
115	$TiCrZrMoHfB_2$	7177.51301	0.36364	1.72429	9	17.90465
116	$TiVCrNbHfB_2$	7144.89048	0.36364	1.68714	9	17.83780
117	$VZrNbMoHfB_2$	7028.47053	0.36364	1.72857	9	17.68137
118	$TiVCrNbMoB_2$	7613.03079	0.59375	1.81000	9	17.10717
119	$TiVCrZrMoB_2$	7442.99015	0.54839	1.77143	9	17.01890
120	$TiVZrNbMoB_2$	7309.24723	0.53333	1.76286	9	17.01890
121	$TiCrZrNbMoB_2$	7442.99015	0.58065	1.76714	9	17.01890
122	$VCrZrNbMoB_2$	7422.79970	0.59375	1.78000	9	17.01890
123	$VCrZrMoHfB_2$	7157.92464	0.37778	1.73714	9	16.88439
124	$VCrZrNbTaB_2$	7190.59674	0.37778	1.68571	9	16.88250
125	$CrZrNbMoHfB_2$	7157.92464	0.40000	1.73286	9	16.34109
126	$TiVCrZrNbB_2$	7243.13055	0.53333	1.69143	9	15.63762

Reference

[1] Gu, J., et al., Dense and pure high-entropy metal diboride ceramics sintered from self-synthesized powders via boro/carbothermal reduction approach. *Sci China Mater* **62,** 1898-1909 (2019).

[2] Feng, L., Fahrenholtz, W.G. & Hilmas, G.E., Processing of dense high-entropy boride ceramics. *J Eur Ceram Soc* **40,** 3815-3823 (2020).

[3] Feng, L., Fahrenholtz, W.G., Hilmas, G.E. & Monteverde, F., Effect of Nb content on the phase composition, densification, microstructure, and mechanical properties of high-entropy boride ceramics. *J Eur Ceram Soc* **41,** 92-100 (2021).

[4] Ma, M., et al., High-pressure sintering of ultrafine-grained high-entropy diboride ceramics. *J Am Ceram Soc* **103,** 6655-6658 (2020).

[5] Liu, J.-X., et al., Mechanical properties of hot-pressed high-entropy diboride-based ceramics. *J Adv Ceram* **9,** 503-510 (2020).

[6] Feng, L., Monteverde, F., Fahrenholtz, W.G. & Hilmas, G.E., Superhard high-entropy AlB_2-type diboride ceramics. *Scr Mater* **199,** 113855 (2021).

[7] Zhang, Y., et al., Microstructure and mechanical properties of high-entropy borides derived from boro/carbothermal reduction. *J Eur Ceram Soc* **39,** 3920-3924 (2019).

[8] Zhang, Y., et al., Dense high-entropy boride ceramics with ultra-high hardness. *Scr Mater* **164,** 135–139 (2019).

[9] Gild, J., et al., Thermal conductivity and hardness of three single-phase high-entropy metal diborides fabricated by borocarbothermal reduction and spark plasma sintering. *Ceram Int* **46,** 6906-6913 (2020).

[10] Li, M., et al., Oscillatory pressure sintering of high entropy $(Zr_{0.2}Ta_{0.2}Nb_{0.2}Hf_{0.2}Mo_{0.2})B_2$ ceramic. *Ceram Int* **47,** 8707-8710 (2021).

[11] Zhang, X., et al., Ultra-incompressible high-entropy diborides. *J Phys Chem Lett* **12,** 3106-3113 (2021).

[12] Akopov, G., Yeung, M.T. & Kaner, R.B., Rediscovering the Crystal Chemistry of Borides. *Adv Mater* **29,** 1604506 (2017).

[13] Ivan'ko, A.A. & Samsonov, G.V. *Handbook of hardness data* (IPST Press, Jerusalem, 1971).

[14] Ni, D.-W., Zhang, G.-J., Kan, Y.-M. & Wang, P.-L., Hot Pressed HfB_2 and HfB_2-20 vol%SiC Ceramics Based on HfB_2Powder Synthesized by Borothermal Reduction of HfO_2*. *Int J Appl Ceram Technol* **7,** 830-836 (2010).

[15] Sairam, K., et al., Reaction spark plasma sintering of niobium diboride. *Int J Refract Met Hard Mater* **43,** 259-262 (2014).

[16] Zapata-Solvas, E., et al., Mechanical properties of ZrB_2- and HfB_2-based ultra-high temperature ceramics fabricated by spark plasma sintering. *J Eur Ceram Soc* **33,** 1373-1386 (2013).

[17] Nakamori, F., et al., Mechanical and thermal properties of bulk ZrB_2. *J Nucl Mater* **467,** 612-617 (2015).

[18] Samsonov, G.V. & Morozov, V.V., Physicochemical properties and structure of simple and complex hydrides of the transition metals. *Sov powder metall met ceram* **9,** 659-664 (1970).

[19] Gild, J., et al., High-entropy metal diborides: a new class of high-entropy materials and a new type of ultrahigh temperature ceramics. *Sci Rep* **6,** 37946 (2016).

[20] Chakraborty, S., Debnath, D., Mallick, A.R. & Das, P.K., Mechanical, tribological, and thermal properties of hot-pressed ZrB_2-B_4C composite. *Int J Appl Ceram Technol* **12,** 568-576 (2015).

[21] Chakraborty, S., Debnath, D., Mallick, A.R. & Das, P.K., Mechanical and thermal properties of hot pressed ZrB_2 system with TiB_2. *Int J Refract Met Hard Mater* **46,** 35-42 (2014).

[22] J, M.-M.N.J., A, D.N.-R.G. & F, M., Characterisation and high temperature mechanical properties of zirconium boride-based materials. *J Eur Ceram Soc* **22,** 2543-2549 (2002).

[23] Shahedi Asl, M., Ghassemi Kakroudi, M., Nayebi, B. & Nasiri, H., Taguchi analysis on the effect of hot pressing parameters on density and hardness of zirconium diboride. *Int J Refract Met Hard Mater* **50,** 313-320 (2015).

[24] Shahedi Asl, M. & Ghassemi Kakroudi, M., Characterization of hot-pressed graphene reinforced ZrB_2–SiC composite. *Mater Sci Eng, A* **625,** 385-392 (2015).

[25] Ma, T., et al., Ultrastrong boron frameworks in ZrB_{12} : A highway for electron conducting. *Adv Mater* **29,** 1-7 (2017).

[26] Akopov, G., et al., Superhard mixed transition metal dodecaborides. *Chem Mater* **28,** 6605-6612 (2016).

[27] Samsonov, G.V., Reactions of Ti, Zr, and W borides with their carbides. *Voprosy Poroshkovoi Met i Prochnosti Materialov, Akad Nauk Ukr SSR* **20,** 72-98 (1959).

[28] Zhang, X., Hilmas, G.E. & Fahrenholtz, W.G., Synthesis, densification, and mechanical properties of TaB_2. *Mater Lett* **62,** 4251-4253 (2008).

[29] Licheri, R., Orrù, R., Musa, C. & Cao, G., Synthesis, densification and characterization of TaB_2–SiC composites. *Ceram Int* **36,** 937-941 (2010).

[30] Chen, H., et al., Hardness measurements for high-pressure prepared TaB and nano-TaC ceramics. *Results Phys* **7,** 3859-3862 (2017).

[31] Mishra, S.K., Rupa, P.K.P. & Pathak, L.C., Surface and nanoindentation studies on nanocrystalline titanium diboride thin film deposited by magnetron sputtering. *Thin Solid Films* **515,** 6884-6889 (2007).

[32] Portnoi, K.I., Samsonov, G.V. & Frolova, K.I., Properties of compacts prepared with titanium boride and the double boride of titanium and chromium with boron carbide. *Zhur Priklad Khim* **33,** 1-7 (1960).

[33] Mukhopadhyay, A., Raju, G.B., Basu, B. & Suri, A.K., Correlation between phase evolution, mechanical properties and instrumented indentation response of TiB_2-based ceramics. *J Eur Ceram Soc* **29,** 505-516 (2009).

[34] Bhaumik, S.K., Divakar, C., Singh, A.K. & Upadhyaya, G.S., Synthesis and sintering of TiB_2 and TiB_2–TiC composite under high pressure. *Mater Sci Eng, A* **279,** 275-281 (2000).

[35] Wang, S., et al., Crystal structures, elastic properties, and hardness of high-pressure synthesized CrB_2 and CrB_4. *J Superhard Mater* **36,** 279-287 (2014).

[36] Han, L., et al., Hardness, elastic, and electronic properties of chromium monoboride. *Appl Phys Lett* **106,** 1-4 (2015).

[37] Samsonov, G., Serebryakova, T. & Neronov, V., Borides. *Sov powder metall met ceram* **5,** 1-10 (1975).

[38] Chen, Y., et al., Ultrasonic and hardness measurements for ultrahigh pressure prepared WB ceramics. *Int J Refract Met Hard Mater* **29,** 329-331 (2011).

[39] Rau, J.V., et al., Superhard tungsten tetraboride films prepared by pulsed laser deposition method. *ACS Appl Mater Interfaces* **3,** 3738-3743 (2011).

[40] Wang, C., et al., WB_2: not a superhard material for strong polarization character of interlayer W-B bonding. *Phys Chem Chem Phys* **19,** 8919-8924 (2017).

[41] Yin, S., et al., Hardness and elastic moduli of high pressure synthesized MoB_2 and WB_2 compacts. *High Pressure Res* **33,** 409-417 (2013).

[42] Tao, Q., et al., Exploring hardness and the distorted sp^2 hybridization of B–B bonds in WB_3. *Chem Mater* **26,** 5297-5302 (2014).

[43] Lundstroem, T., The structure of Ru_2B_3 and WB_2 as determined by single-crystal diffractometry, and some notes on the W-B system. *Key Eng Mater* **30,** 115-127 (1969).

[44] Bodrova, L.G., Koval'chenko, M.S. & Serebryakova, T.I., Preparation of tungsten tetraboride. *Sov powder metall met ceram* **13,** 1-3 (1974).

[45] Mohammadi, R., et al., Tungsten tetraboride, an inexpensive superhard material. *PNAS* **108,** 10958-62 (2011).

[46] Gu, Q., Krauss, G. & Steurer, W., Transition metal borides: superhard versus ultra-incompressible. *Adv Mater* **20,** 3620-3626 (2008).

[47] Portnoi, K.I., et al., Phase diagram of the molybdenum-boron system. *Izv Akad Nauk SSSR, Metal* **4,** 171-176 (1967).

[48] Chung, H.-Y., Yang, J.M., Tolbert, S.H. & Kaner, R.B., Anisotropic mechanical properties of ultra-incompressible, hard osmium diboride. *J Mater Res* **23,** 1797-1801 (2008).

[49] Wang, P., et al., Vanadium diboride (VB_2) synthesized at high pressure: elastic, mechanical, electronic, and magnetic properties and thermal stability. *Inorg Chem* **57,** 1096-1105 (2018).

[50] Chung, H.Y., et al., Synthesis of ultra-incompressible superhard rhenium diboride at ambient pressure. *Science* **316,** 436-439 (2007).

[51] Levine, J.B., et al., Preparation and properties of metallic, superhard rhenium diboride crystals. *J Am Chem Soc* **130,** 16953-16958 (2008).

[52] Weinberger, M.B., et al., Incompressibility and hardness of solid solution transition metal diborides: $Os_{1-x}Ru_xB_2$. *Chem Mater* **21,** 1915-1921 (2009).

[53] Akopov, G., et al., Investigation of hardness of ternary borides of the $YCrB_4$, Y_2ReB_6, Y_3ReB_7, and YMo_3B_7 structural types. *Chem Mater* **30,** 6494-6502 (2018).

[54] Carlsson, J.O. & Lundström, T., The solution hardening of β-rhombohedral boron. *J Less-Common Met* **22,** 317-320 (1970).

[55] Portnoi, K.I. & Romashov, V.M., Binary constitution diagrams of systems composed of various elements and boron - a review. *Sov powder metall met ceram* **11,** 378-384 (1972).

[56] Bolgar, A.S., et al., High-temperature enthalpy and heat capacity of borides of the niobium-boron system. *Sov powder metall met ceram* **22,** 207-211 (1983).

[57] Odintsov, V.V., Hardness of metal dodecaborides with the UB_{12} type structure. *Izv Akad Nauk SSSR, Neorg Mater* **10,** 366-367 (1974).